

Port-Hamiltonian flexible multibody dynamics

Andrea Brugnoli¹ · Daniel Alazard¹ ·
Valérie Pommier-Budinger¹ · Denis
Matignon¹

Received: date / Accepted: date

Abstract A new formulation for the modular construction of multibody systems is presented. By rearranging the classical model for a flexible floating body and introducing the appropriate canonical momenta, the model is recast into a coupled system of ordinary and partial differential equations in port-Hamiltonian form. This approach relies on a floating frame description and stays valid under the assumption of small deformations. A finite element based method is then introduced to discretize the dynamics in a structure preserving manner. Joints are introduced by interconnecting each body to the surrounding elements in a modular way. Constraints are imposed on a velocity level, leading to an index 2 quasi linear differential-algebraic system. Model reduction techniques are readily available for the linearized dynamics. Numerical tests are carried out to assess the validity of the proposed approach.

Keywords Port-Hamiltonian systems · Floating frame formulation · Flexible multibody system · Structure preserving discretization

This work is supported by the project ANR-16-CE92-0028, entitled *Interconnected Infinite-Dimensional systems for Heterogeneous Media*, INFIDHEM, financed by the French National Research Agency (ANR) and the Deutsche Forschungsgemeinschaft (DFG). Further information is available at <https://websites.isae-supaero.fr/infidhem/the-project>.

Andrea Brugnoli
E-mail: andrea.brugnoli@isae.fr

Daniel Alazard
E-mail: daniel.alazard@isae.fr

Valérie Pommier-Budinger
E-mail: valerie.budinger@isae.fr

Denis Matignon
E-mail: denis.matignon@isae.fr

¹ISAE-SUPAERO, Université de Toulouse, France.
10 Avenue Edouard Belin, BP-54032, 31055 Toulouse Cedex 4.

1 Introduction

Especially in aerospace application, where a strict requirement for lightweight structures applies, the accurate modeling of flexible multibody system is increasingly important. For structural control co-design, it is of interest to lower the system complexity and to dispose of a modular description, to simplify analysis. In this spirit, the transfer matrix method [28] and the component mode synthesis [17] are two well known substructuring techniques that allow the construction of complex multibody systems by interconnecting simpler models. These methodologies have been refined for structural and control co-design. A reformulation of the Finite Element-Transfer Matrix (FE-TM) method [32] allows an easy construction of reduced models that are suited for decentralized control design. For the component mode synthesis, the controlled component synthesis (CCS) has been proposed in [35], a framework for the design of decentralized controller of flexible structures.

To incorporate the elastic motion in multibody systems, three description are commonly used: the floating frame formulation, the corotational frame formulation and the inertial frame formulation [14]. The corotational and inertial frame formulations allow to take into account large deformations of the elastic body but the application of linear model reduction techniques remains impractical [33]. On the contrary, the floating frame formulation, relying on the hypothesis of small deformations, integrates easily many model reduction techniques [25], making it possible to obtain a low-dimensional problem that can be exploited for control design.

The Lagrangian formulation is the most commonly used methodology to retrieve the equations of motion. However, the port-Hamiltonian (pH) framework [12] has been recently extended to describe the dynamics of rigid and flexible links [21, 22]. The definition of the model naturally accounts for the non-linearities due to large deformations. Thanks to the properties of pH systems [9], this approach allows for the modular construction by interconnecting simpler elements. Nevertheless, the formulation therein heavily relies on Lie algebra and differential geometry concepts, making the overall implementation and understanding difficult. Furthermore, the discretization of underlying PDE requires non standard methodologies [16].

In this paper, the pH formulation of flexible multibody system is constructed using a floating frame approach. Starting from the general equation for the rigid flexible dynamics of a floating body [29], an equivalent port-Hamiltonian system is found by appropriate selection of the canonical momenta. The flexible behavior is based on the linear elasticity assumption making it possible to include models that cannot be easily formulated in terms of differential form [5, 6]. The problem is then written as a coupled system of ODEs and PDEs, extending the general definition of finite-dimensional port-Hamiltonian descriptor systems provided in [23]. A suitable structure preserving discretization method, based on [8], is then used to obtain a finite dimensional pH system. Each individual component can then be interconnected to the other bodies using standard interconnection of pH system, as it is done in [22]. The constraints are imposed on the velocities and results in a quasi-linear index 2 differential-algebraic port-Hamiltonian system (pHDAE) [31]. The algebraic constraints can be eliminated, preserving the overall pH structure, using standard null space methods [20]. The modularity feature of pH system

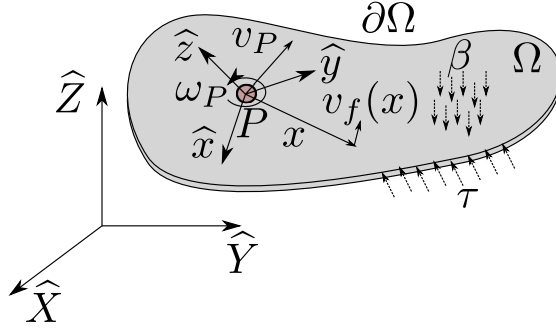


Fig. 1 Thin floating body undergoing a surface traction τ and body force density β

makes the proposed approach analogous to a substructuring technique [19]. A complex multibody system can be assembled by interconnecting blocks, allowing the usage of modeling platform like SIMULINK[®]. As a floating frame formulation is used, model reduction technique can be employed to lower the computational complexity of the model [10,13]. All the features make the proposed formulation interesting for control applications, that can benefit from the properties of pH systems [26,24].

The paper is organized in the following manner. In Section 2 the classical equations of a flexible floating body, derived by means of the virtual work principle [29, 30], are recalled. Using the Jacobi identity the equations are recast in a form closer to the pH structure. Section 3 details the pH formulation of a floating flexible body by introducing the proper canonical momenta. Once a generic potential energy is introduced, the final formulation is then obtained. In Section 4 a finite element based discretization is detailed for the elastodynamics problem. The procedure is then easily applied to flexible floating bodies. The particular case of thin planar beams is then detailed, as it will be then employed in the simulation part. Section 5 explains how to interconnect models together using classical pH interconnection. A revolute joint connection is taken as example, as it will be Section 6 is devoted to numerical examples, to assess the validity of the proposed. The test cases are taken from previously published articles.

2 Flexible dynamics of a floating body

The coupled ODE-PDE system representing the motion of a single flexible body are here recalled. Consider an open connected set $\Omega \in \mathbb{R}^3$, representing a floating flexible body. The dynamics is computed at a generic point P , that is not necessarily the center of mass. The velocity of a generic point is expressed by considering a small flexible displacement superimposed to the rigid motion

$$\mathbf{v} = \mathbf{v}_P + [\boldsymbol{\omega}_P]_{\times}(\mathbf{x} + \mathbf{u}_f) + \mathbf{v}_f,$$

where $\mathbf{v}_P, \boldsymbol{\omega}_P$ is the linear and angular velocities of point P and $\mathbf{v}_f := \dot{\mathbf{u}}_f$ is the time derivative of the deformation displacement \mathbf{u}_f (computed in the body frame). These quantities are evaluated in the body reference frame $\hat{\mathbf{x}}, \hat{\mathbf{y}}, \hat{\mathbf{z}}$ (see Fig. 1). The notation $[\mathbf{a}]_{\times}$ denotes the skew-symmetric matrix associated to vector \mathbf{a} .

The model for the classical equations derived using the principle of virtual work can be found in [29, 30]. The small difference with respect to the derivation therein is that the equation for the translation is now written in the body frame.

Linear momentum balance:

$$\begin{aligned} m(\dot{\mathbf{v}}_P + [\boldsymbol{\omega}_P]_{\times} \mathbf{v}_P) + [\mathbf{s}_u]_{\times}^{\top} \dot{\boldsymbol{\omega}}_P + \int_{\Omega} \rho \ddot{\mathbf{u}}_f \, d\Omega = \\ - [\boldsymbol{\omega}_P]_{\times} [\boldsymbol{\omega}_P]_{\times} \mathbf{s}_u - \int_{\Omega} 2\rho [\boldsymbol{\omega}_P]_{\times} \dot{\mathbf{u}}_f \, d\Omega + \int_{\Omega} \boldsymbol{\beta} \, d\Omega + \int_{\partial\Omega} \boldsymbol{\tau} \, d\Gamma. \end{aligned} \quad (1)$$

Angular momentum balance:

$$\begin{aligned} [\mathbf{s}_u]_{\times} (\dot{\mathbf{v}}_P + [\boldsymbol{\omega}_P]_{\times} \mathbf{v}_P) + \mathbf{J}_u \dot{\boldsymbol{\omega}}_P + \int_{\Omega} \rho [\mathbf{x} + \mathbf{u}_f]_{\times} \ddot{\mathbf{u}}_f \, d\Omega - [\boldsymbol{\omega}_P]_{\times} \mathbf{J}_u \boldsymbol{\omega}_P = \\ - \int_{\Omega} 2\rho [\mathbf{x} + \mathbf{u}_f]_{\times} [\boldsymbol{\omega}_P]_{\times} \dot{\mathbf{u}}_f \, d\Omega + \int_{\Omega} [\mathbf{x} + \mathbf{u}_f]_{\times} \boldsymbol{\beta} \, d\Omega + \int_{\partial\Omega} [\mathbf{x} + \mathbf{u}_f]_{\times} \boldsymbol{\tau} \, d\Gamma. \end{aligned} \quad (2)$$

Flexibility PDE:

$$\rho(\dot{\mathbf{v}}_P + [\boldsymbol{\omega}_P]_{\times} \mathbf{v}_P) + \rho([\dot{\boldsymbol{\omega}}_P]_{\times} + [\boldsymbol{\omega}_P]_{\times} [\boldsymbol{\omega}_P]_{\times})(\mathbf{x} + \mathbf{u}_f) + \rho(2[\boldsymbol{\omega}_P]_{\times} \dot{\mathbf{u}}_f + \ddot{\mathbf{u}}_f) = \text{Div } \boldsymbol{\Sigma} + \boldsymbol{\beta}, \quad (3)$$

where ρ is the mass density, $m = \int_{\Omega} \rho \, d\Omega$ is the total mass, $\mathbf{s}_u = \int_{\Omega} \rho(\mathbf{x} + \mathbf{u}_f) \, d\Omega$ is the static moment, $\mathbf{J}_u = - \int_{\Omega} \rho[\mathbf{x} + \mathbf{u}_f]_{\times} [\mathbf{x} + \mathbf{u}_f]_{\times} \, d\Omega$ is the inertia matrix. Variable $\boldsymbol{\Sigma}$ is the Cauchy stress tensor. From linear elasticity theory it is well known that the infinitesimal stress is given by $\boldsymbol{\varepsilon} = \text{Grad}(\mathbf{u}_f)$, where $\text{Grad} = \frac{1}{2}[\nabla + \nabla^{\top}]$. The constitutive equation is expressed as $\boldsymbol{\Sigma} = \boldsymbol{\mathcal{D}}\boldsymbol{\varepsilon}$, where $\boldsymbol{\mathcal{D}}$ is the stiffness tensor. Additionally, $\boldsymbol{\beta}$ is a density force and $\boldsymbol{\tau}$ is a surface traction, both expressed in the body reference frame.

Considering that $\dot{\mathbf{v}}_f = \ddot{\mathbf{u}}_f$ and using the Jacobi identity (see Appendix 1) Eqs. (1), (2), (3) can be rewritten in an equivalent way.

Linear momentum balance:

$$\begin{aligned} m\dot{\mathbf{v}}_P + [\mathbf{s}_u]_{\times}^{\top} \dot{\boldsymbol{\omega}}_P + \int_{\Omega} \rho \dot{\mathbf{v}}_f \, d\Omega = \\ \left[m\mathbf{v}_P + [\mathbf{s}_u]_{\times}^{\top} \boldsymbol{\omega}_P + 2 \int_{\Omega} \rho \mathbf{v}_f \, d\Omega \right]_{\times} \boldsymbol{\omega}_P + \int_{\Omega} \boldsymbol{\beta} \, d\Omega + \int_{\partial\Omega} \boldsymbol{\tau} \, d\Gamma. \end{aligned} \quad (4)$$

Angular momentum balance:

$$\begin{aligned} [\mathbf{s}_u]_{\times} \dot{\mathbf{v}}_P + \mathbf{J}_u \dot{\boldsymbol{\omega}}_P + \int_{\Omega} \rho [\mathbf{x} + \mathbf{u}_f]_{\times} \dot{\mathbf{v}}_f \, d\Omega = \\ \left[[\mathbf{s}_u]_{\times}^{\top} \boldsymbol{\omega}_P + 2 \int_{\Omega} \rho \mathbf{v}_f \, d\Omega \right]_{\times} \mathbf{v}_P + \left[[\mathbf{s}_u]_{\times} \mathbf{v}_P + \mathbf{J}_u \boldsymbol{\omega}_P + 2 \int_{\Omega} \rho [\mathbf{x} + \mathbf{u}_f]_{\times} \mathbf{v}_f \, d\Omega \right]_{\times} \boldsymbol{\omega}_P + \\ 2 \int_{\Omega} \left[\rho \mathbf{v}_P + \rho [\mathbf{x} + \mathbf{u}_f]_{\times}^{\top} \boldsymbol{\omega}_P \right]_{\times} \mathbf{v}_f \, d\Omega + \int_{\Omega} [\mathbf{x} + \mathbf{u}_f]_{\times} \boldsymbol{\beta} \, d\Omega + \int_{\partial\Omega} [\mathbf{x} + \mathbf{u}_f]_{\times} \boldsymbol{\tau} \, d\Gamma. \end{aligned} \quad (5)$$

Flexibility PDE:

$$\begin{aligned} \rho \dot{\mathbf{v}}_P + \rho [\mathbf{x} + \mathbf{u}_f]_{\times}^{\top} \dot{\boldsymbol{\omega}}_P + \rho \dot{\mathbf{v}}_f = \\ \left[\rho \mathbf{v}_P + \rho [\mathbf{x} + \mathbf{u}_f]_{\times}^{\top} \boldsymbol{\omega}_P + 2\rho \mathbf{v}_f \right]_{\times} \boldsymbol{\omega}_P + \text{Div } \boldsymbol{\Sigma} + \boldsymbol{\beta}. \end{aligned} \quad (6)$$

Equation (6) requires the specification of the boundary conditions

$$\begin{aligned}\boldsymbol{\Sigma} \cdot \mathbf{n}|_{\Gamma_N} &= \boldsymbol{\tau}|_{\Gamma_N}, \quad \mathbf{n} \text{ is the outward normal,} \\ \mathbf{u}_f|_{\Gamma_D} &= \bar{\mathbf{u}}_f|_{\Gamma_D},\end{aligned}\tag{7}$$

where the boundary $\partial\Omega = \Gamma_D \cup \Gamma_N$ has been split into two subset for the Neumann and Dirichlet boundary conditions. By introduction of the appropriate momenta this model can be reformulated as pH system as illustrated in the following section.

3 PH formulation

In this section the flexible dynamics of a floating body is written as a coupled system of ODEs and PDEs in pH form. The final form is a descriptor port-Hamiltonian system that fits and generalizes the framework detailed in [23].

Consider the total energy (Hamiltonian), given by the sum of kinetic, elastic and potential energy:

$$\begin{aligned}H &= H_{\text{kin}} + H_{\text{def}} + H_{\text{pot}} \\ &= \frac{1}{2} \int_{\Omega} \left\{ \rho \|\mathbf{v}_P + [\boldsymbol{\omega}_P]_{\times}(\mathbf{x} + \mathbf{u}_f) + \mathbf{v}_f\|^2 + \boldsymbol{\Sigma} : \boldsymbol{\varepsilon} \right\} d\Omega + H_{\text{pot}}.\end{aligned}\tag{8}$$

The inner product $\mathbf{A} : \mathbf{B} = \text{Tr}(\mathbf{A}\mathbf{B}^T)$ is the tensor contraction. The momenta (usually called energy variables in the pH framework) are then computed by derivation of the Hamiltonian. As the variables belong to finite- and infinite-dimensional spaces the derivative is either a classical gradient either a variational derivative:

$$\begin{aligned}\mathbf{p}_t &:= \frac{\partial H}{\partial \mathbf{v}_P} = m\mathbf{v}_P + [\mathbf{s}_u]_{\times}^{\top} \boldsymbol{\omega}_P + \int_{\Omega} \rho \mathbf{v}_f d\Omega, \\ \mathbf{p}_r &:= \frac{\partial H}{\partial \boldsymbol{\omega}_P} = [\mathbf{s}_u]_{\times} \mathbf{v}_P + \mathbf{J}_u \boldsymbol{\omega}_P + \int_{\Omega} \rho [\mathbf{x} + \mathbf{u}_f]_{\times} \mathbf{v}_f d\Omega, \\ \mathbf{p}_f &:= \frac{\delta H}{\delta \mathbf{v}_f} = \rho \mathbf{v}_P + \rho [\mathbf{x} + \mathbf{u}_f]_{\times}^{\top} \boldsymbol{\omega}_P + \rho \mathbf{v}_f, \\ \boldsymbol{\varepsilon} &:= \frac{\delta H}{\delta \boldsymbol{\Sigma}} = \boldsymbol{\mathcal{D}}^{-1} \boldsymbol{\Sigma}.\end{aligned}\tag{9}$$

The relation between energy and co-energy variable is then given by

$$\begin{bmatrix} \mathbf{p}_t \\ \mathbf{p}_r \\ \mathbf{p}_f \\ \boldsymbol{\varepsilon} \end{bmatrix} = \underbrace{\begin{bmatrix} m\mathbf{I}_{3 \times 3} & [\mathbf{s}_u]_{\times}^{\top} & \mathcal{I}_{\rho}^{\Omega} & 0 \\ [\mathbf{s}_u]_{\times} & \mathbf{J}_u & \mathcal{I}_{\rho x}^{\Omega} & 0 \\ (\mathcal{I}_{\rho}^{\Omega})^* & (\mathcal{I}_{\rho x}^{\Omega})^* & \rho & 0 \\ 0 & 0 & 0 & \boldsymbol{\mathcal{D}}^{-1} \end{bmatrix}}_{\boldsymbol{\mathcal{M}}: \text{Mass operator}} \begin{bmatrix} \mathbf{v}_P \\ \boldsymbol{\omega}_P \\ \mathbf{v}_f \\ \boldsymbol{\Sigma} \end{bmatrix},\tag{10}$$

where $\mathbf{I}_{3 \times 3}$ is the identity matrix in \mathbb{R}^3 . and the operators are defined as

$$\begin{aligned}\mathcal{I}_{\rho}^{\Omega} &:= \int_{\Omega} \rho(\cdot) d\Omega, & \mathcal{I}_{\rho x}^{\Omega} &:= \int_{\Omega} \rho[\mathbf{x} + \mathbf{u}_f]_{\times}(\cdot) d\Omega, \\ (\mathcal{I}_{\rho}^{\Omega})^* &:= \rho, & (\mathcal{I}_{\rho x}^{\Omega})^* &:= \rho[\mathbf{x} + \mathbf{u}_f]_{\times}^{\top}.\end{aligned}$$

The superscript $*$ denotes the adjoint operator. The mass operator \mathcal{M} is a self-adjoint, positive operator. The kinetic and deformation energy can then be written as

$$H_{\text{kin}} + H_{\text{def}} = \frac{1}{2} \langle \mathbf{e}_{\text{kd}}, \mathcal{M} \mathbf{e}_{\text{kd}} \rangle \quad (11)$$

where $\mathbf{e}_{\text{kd}} = [\mathbf{v}_P; \boldsymbol{\omega}_P; \mathbf{v}_f; \boldsymbol{\Sigma}]$ and the scalar product $\langle \cdot, \cdot \rangle$ is taken over the space $\mathbb{R}^3 \times \mathbb{R}^3 \times \mathcal{L}^2(\Omega, \mathbb{R}^3) \times \mathcal{L}^2(\Omega, \mathbb{R}^{3 \times 3})$ (\mathcal{L}^2 is the space of square integrable functions). It is important to notice that the kinetic energy also depends on the flexible displacement:

$$\frac{\delta H_{\text{kin}}}{\delta \mathbf{u}_f} = [\mathbf{p}_f]_{\times} \boldsymbol{\omega}_P$$

In order to get a complete formulation generalized coordinates are required. Those are:

- ${}^i \mathbf{r}_P$: the position of point P in the inertial frame of reference;
- \mathbf{R} : the orientation matrix that transforms vectors from the body frame to the inertial frame (other attitude parametrization are possible, here the orientation matrix is considered for ease of presentation);
- \mathbf{u}_f the flexible displacement;

In particular, following [15], the orientation matrix is converted in a vector by concatenating its rows

$$\mathbf{R}_v = \text{vec}(\mathbf{R}^\top) = [\mathbf{R}_x \ \mathbf{R}_y \ \mathbf{R}_z]^\top,$$

where $\mathbf{R}_x, \mathbf{R}_y, \mathbf{R}_z$ are the first, second and third row of matrix \mathbf{R} . Furthermore the corresponding cross map will be given by

$$[\mathbf{R}_v]_{\times} = \begin{bmatrix} [\mathbf{R}_x]_{\times} \\ [\mathbf{R}_y]_{\times} \\ [\mathbf{R}_z]_{\times} \end{bmatrix} \quad [\mathbf{R}_v]_{\times} : \mathbb{R}^9 \rightarrow \mathbb{R}^{9 \times 3}$$

The overall port Hamiltonian formulation is then (omitting the external forces and torques)

$$\underbrace{\begin{bmatrix} \mathbf{I}_1 & 0 \\ 0 & \mathcal{M} \end{bmatrix}}_{\boldsymbol{\varepsilon}} \frac{d}{dt} \underbrace{\begin{bmatrix} {}^i \mathbf{r}_P \\ \mathbf{R}_v \\ \mathbf{u}_f \\ \mathbf{v}_P \\ \boldsymbol{\omega}_P \\ \mathbf{v}_f \\ \boldsymbol{\Sigma} \end{bmatrix}}_e = \underbrace{\begin{bmatrix} 0 & 0 & 0 & \mathbf{R} & 0 & 0 & 0 \\ 0 & 0 & 0 & 0 & [\mathbf{R}_v]_{\times} & 0 & 0 \\ 0 & 0 & 0 & 0 & 0 & \mathbf{I}_{3 \times 3} & 0 \\ -\mathbf{R}^\top & 0 & 0 & 0 & [\tilde{\mathbf{p}}_t]_{\times} & 0 & 0 \\ 0 & -[\mathbf{R}_v]_{\times}^\top & 0 & [\tilde{\mathbf{p}}_t]_{\times} & [\tilde{\mathbf{p}}_r]_{\times} & \boldsymbol{\mathcal{I}}_{p_f}^\Omega & 0 \\ 0 & 0 & -\mathbf{I}_{3 \times 3} & 0 & -(\boldsymbol{\mathcal{I}}_{p_f}^\Omega)^* & 0 & \text{Div} \\ 0 & 0 & 0 & 0 & 0 & \text{Grad} & 0 \end{bmatrix}}_{\mathcal{J}} \underbrace{\begin{bmatrix} \partial_{\mathbf{r}_P} H \\ \partial_{\mathbf{R}_v} H \\ \delta_{\mathbf{u}_f} H \\ \mathbf{v}_P \\ \boldsymbol{\omega}_P \\ \mathbf{v}_f \\ \boldsymbol{\Sigma} \end{bmatrix}}_z, \quad (12)$$

Variables $\tilde{\mathbf{p}}_t, \tilde{\mathbf{p}}_r$ are defined as

$$\begin{aligned} \tilde{\mathbf{p}}_t &= \mathbf{p}_t + \int_{\Omega} \rho \mathbf{v}_f \, d\Omega, \\ \tilde{\mathbf{p}}_r &= \mathbf{p}_r + \int_{\Omega} \rho [\mathbf{x} + \mathbf{u}_f]_{\times} \mathbf{v}_f \, d\Omega. \end{aligned} \quad (13)$$

The operator $\mathcal{I}_{p_f}^\Omega$ is defined as

$$\mathcal{I}_{p_f}^\Omega := \int_{\Omega} \{2[\mathbf{p}_f]_{\times} + \rho[\mathbf{v}_f]_{\times}\}(\cdot) \, d\Omega.$$

Its formal adjoint is given by $(\mathcal{I}_{p_f}^\Omega)^* = -\{2[\mathbf{p}_f]_{\times} + \rho[\mathbf{v}_f]_{\times}\}(\cdot)$. The 2 coefficient is required to compensate the contribution given by $\delta_{\mathbf{u}_f}H$. The additional terms related to $\rho\mathbf{v}_f$ are associated to the coriolis accelerations that affect the deformation field. It is important to highlight that Div and Grad are formally skew-adjoint operators, i.e. for homogeneous boundary conditions (I.B.P. stays for integration by parts)

$$\begin{aligned} \int_{\Omega} \boldsymbol{\Sigma} : \text{Grad}(\mathbf{v}_f) \, d\Omega &\stackrel{\text{I.B.P.}}{=} - \int_{\Omega} \text{Div}(\boldsymbol{\Sigma}) \cdot \mathbf{v}_f \, d\Omega, \\ \langle \boldsymbol{\Sigma}, \text{Grad}(\mathbf{v}_f) \rangle_{\mathcal{L}^2(\Omega, \mathbb{R}_{\text{sym}}^{d \times d})} &\stackrel{\text{I.B.P.}}{=} - \langle \text{Div}(\boldsymbol{\Sigma}), \mathbf{v}_f \rangle_{\mathcal{L}^2(\Omega, \mathbb{R}^d)}, \end{aligned}$$

where $\langle \cdot, \cdot \rangle_{\mathcal{H}}$ denote an inner product over the Hilbert space \mathcal{H} .

$\mathcal{L}^2(\Omega, \mathbb{R}^d)$, $\mathcal{L}^2(\Omega, \mathbb{R}_{\text{sym}}^{d \times d})$ are the spaces of square integrable vector-valued or symmetric tensors-valued functions in a geometric domain of dimension d .

For this reason operator \mathcal{J} is skew-symmetric $\mathcal{J}^* = -\mathcal{J}$.

The potential energy contribution accounts for possible conservative forces. For example if a gravity force is considered, the corresponding potential reads

$$H_{\text{pot}} = \int_{\Omega} \rho g \, {}^i r_z \, d\Omega = \int_{\Omega} \rho g \left[{}^i r_{P,z} + \mathbf{R}_z(\mathbf{x} + \mathbf{u}_f) \right] \, d\Omega.$$

The associated co-energy variables are easily obtained

$$\begin{aligned} \partial_{\mathbf{r}_P} H_{\text{pot}} &= mg \, \widehat{\mathbf{Z}}, \quad \widehat{\mathbf{Z}} \text{ is the inertial frame vertical direction} \\ \partial_{\mathbf{R}_v} H_{\text{pot}} &= [\mathbf{0}_{(3,1)}, \mathbf{0}_{(3,1)}, \int_{\Omega} \rho g (\mathbf{x} + \mathbf{u}_f)^{\top} \, d\Omega]^{\top} \\ \delta_{\mathbf{u}_f} H_{\text{pot}} &= \rho g \, \mathbf{R}_z^{\top} \end{aligned}$$

These correspond to the forcing terms due to gravity. System (12) fits into the framework detailed in [23] and extends it as a coupled system of ODEs and PDEs is considered. It can be rewritten compactly as follows

$$\begin{aligned} \mathcal{E}(e)\dot{e} &= \mathcal{J}(e)z(e) + \mathcal{B}_d(e)\mathbf{u}_d + \mathcal{B}_r(e)\mathbf{u}_{\partial}, \\ \mathbf{y}_d &= \mathcal{B}_d^*(e)z(e), \\ \mathbf{u}_{\partial} &= \mathcal{B}_{\partial}z(e) = [\boldsymbol{\Sigma} \cdot \mathbf{n}|_{\Gamma_N}, \partial_t \mathbf{u}_f|_{\Gamma_D}], \\ \mathbf{y}_{\partial} &= \mathcal{C}_{\partial}z(e) = [\partial_t \mathbf{u}_f|_{\Gamma_N}, \boldsymbol{\Sigma} \cdot \mathbf{n}|_{\Gamma_D}], \end{aligned} \tag{14}$$

where $\mathbf{u}_d = \boldsymbol{\beta}$, $\mathbf{u}_{\partial} = \boldsymbol{\tau}$. The control operators are expressed as

$$\begin{aligned} \mathcal{B}_d &= [0; 0; 0; \mathcal{I}^\Omega; \mathcal{I}_x^\Omega; \mathbf{I}; 0], \\ \mathcal{B}_r &= [0; 0; 0; \mathcal{I}^\Gamma; \mathcal{I}_x^\Gamma; 0; 0]. \end{aligned}$$

The control operators read

$$\begin{aligned}\mathcal{I}^\Omega &:= \int_\Omega (\cdot) \, d\Omega, & \mathcal{I}_x^\Omega &:= \int_\Omega [\mathbf{x} + \mathbf{u}_f]_\times (\cdot) \, d\Omega, \\ \mathcal{I}^\Gamma &:= \int_{\partial\Omega} (\cdot) \, d\Gamma, & \mathcal{I}_x^\Gamma &:= \int_{\partial\Omega} [\mathbf{x} + \mathbf{u}_f]_\times (\cdot) \, d\Gamma.\end{aligned}$$

The gradient of the Hamiltonian gives $\partial_e H = \mathcal{E}^* \mathbf{z}$. Adopting the same nomenclature as in [23], \mathbf{e} contains the state and \mathbf{z} contains the effort functions. In this case the operators verify $\mathcal{E} = \mathcal{E}^*$, $\mathcal{J} = -\mathcal{J}^*$. The distributed control operator \mathcal{B}_d is bounded. Even if three dimensional elasticity has been taken as example up to this point, simpler models are easily considered. Beam and plate models [5, 6] are described by appropriate differential operators that replace the Div, Grad appearing in (12) (see §4.3).

Remark 1 The linear elasticity hypothesis does not allow to include the effect of non linearities due to large deformations. However, geometric stiffening could be considered by adding a potential energy associated to centrifugal forces [34].

Remark 2 If case of vanishing deformation $\mathbf{u}_f \equiv 0$ the Newton-Euler equations on the Euclidian group $SE(3)$ are retrieved

$$\begin{bmatrix} {}^i\dot{\mathbf{r}}_P \\ \dot{\mathbf{R}}_v \\ \dot{\mathbf{p}}_t \\ \dot{\mathbf{p}}_r \end{bmatrix} = \begin{bmatrix} 0 & 0 & \mathbf{R} & 0 \\ 0 & 0 & 0 & [\mathbf{R}_v]_\times \\ -\mathbf{R}^\top & 0 & 0 & [\mathbf{p}_t]_\times \\ 0 & -[\mathbf{R}]_\times^\top & [\mathbf{p}_t]_\times & [\mathbf{p}_r]_\times \end{bmatrix} \begin{bmatrix} \partial_{\mathbf{r}_P} H \\ \partial_{\mathbf{R}_v} H \\ \mathbf{v}_P \\ \boldsymbol{\omega}_P \end{bmatrix},$$

where

$$\begin{bmatrix} \mathbf{p}_t \\ \mathbf{p}_r \end{bmatrix} = \begin{bmatrix} m\mathbf{I} & [\mathbf{s}]_\times^\top \\ [\mathbf{s}]_\times & \mathbf{J} \end{bmatrix} \begin{bmatrix} \mathbf{v}_P \\ \boldsymbol{\omega}_P \end{bmatrix}, \quad \mathbf{p} = \mathbf{M}\mathbf{v}$$

The kinetic energy is then given by $H_{\text{kin}} = \frac{1}{2} \mathbf{v}^\top \mathbf{M} \mathbf{v}$. This system can be written in standard pH form as $\dot{\mathbf{x}} = \mathbf{J}(\mathbf{x}) \partial_{\mathbf{x}} H$.

4 Discretization procedure

A finite-element based technique to obtain a finite dimensional pH system is illustrated. This methodology relies on the results explained in [8] and boils down to three simple steps

1. The system is put into weak form;
2. An integration by parts is applied to highlight the proper boundary control;
3. A Galerkin method is employed to obtain a finite-dimensional system.

4.1 Illustration for the Elastodynamics PDE

To explain the methodology consider the elastodynamics PDE

$$\rho \frac{\partial^2 \mathbf{u}}{\partial t^2} - \text{Div}(\mathcal{D} \text{Grad}(\mathbf{u})) = \mathbf{u}_d,$$

where a distributed control u_d (a volumetric force) is considered. This model describe the flexible vibrations assuming small deformations. It is embedded in the general formulation (12) and therefore the procedure explained here is easily adapted to the general formulation.

To get a pH representation the energy variables have to properly selected by considering the total energy

$$H = \frac{1}{2} \int_{\Omega} \left\{ \rho \left(\frac{\partial \mathbf{u}}{\partial t} \right)^2 + \boldsymbol{\Sigma} : \boldsymbol{\varepsilon} \right\} d\Omega.$$

Taking as energies the linear momentum and the deformation

$$\begin{aligned} \text{Energies} \quad \mathbf{x}_1 &= \rho \, \partial_t \mathbf{u}, & \mathbf{X}_2 &= \boldsymbol{\varepsilon} = \text{Grad}(\mathbf{u}). \\ \text{Co-energies} \quad \mathbf{e}_1 &:= \frac{\delta H}{\delta \mathbf{x}_1} = \partial_t \mathbf{u}, & \mathbf{E}_2 &:= \frac{\delta H}{\delta \mathbf{X}_2} = \boldsymbol{\Sigma}, \end{aligned} \quad (15)$$

the port-Hamiltonian representation in co-energy variables becomes

$$\underbrace{\begin{bmatrix} \rho & 0 \\ 0 & \mathcal{D}^{-1} \end{bmatrix}}_{\mathcal{M}} \frac{\partial}{\partial t} \underbrace{\begin{bmatrix} \mathbf{e}_1 \\ \mathbf{E}_2 \end{bmatrix}}_{\mathcal{J}} = \underbrace{\begin{bmatrix} 0 & \text{Div} \\ \text{Grad} & 0 \end{bmatrix}}_{\mathcal{J}} \underbrace{\begin{bmatrix} \mathbf{e}_1 \\ \mathbf{E}_2 \end{bmatrix}}_{\mathcal{J}} + \underbrace{\begin{bmatrix} \mathbf{I} \\ 0 \end{bmatrix}}_{\mathcal{B}_d} \mathbf{u}_d$$

The interconnection operator may be decomposed as $\mathcal{J} = \mathcal{J}_{\text{Div}} + \mathcal{J}_{\text{Grad}}$

$$\underbrace{\begin{bmatrix} 0 & \text{Div} \\ \text{Grad} & 0 \end{bmatrix}}_{\mathcal{J}} = \underbrace{\begin{bmatrix} 0 & \text{Div} \\ 0 & 0 \end{bmatrix}}_{\mathcal{J}_{\text{Div}}} + \underbrace{\begin{bmatrix} 0 & 0 \\ \text{Grad} & 0 \end{bmatrix}}_{\mathcal{J}_{\text{Grad}}} \quad (16)$$

Assuming a Neumann boundary conditions (the normal traction $\boldsymbol{\tau}$ is known at the boundary), this system can be written compactly as a boundary control system

$$\begin{aligned} \mathcal{M} \frac{\partial \mathbf{e}}{\partial t} &= \mathcal{J} \mathbf{e} + \mathcal{B}_d \mathbf{u}_d, \\ \mathbf{y}_d &= \mathcal{B}_d^* \mathbf{e}, \\ \mathbf{u}_{\partial} &= [\mathbf{E}_2 \cdot \mathbf{n}|_{\Gamma_N}, \mathbf{e}_1|_{\Gamma_D}], \\ \mathbf{y}_{\partial} &= [\mathbf{e}_1|_{\Gamma_N}, \mathbf{E}_2 \cdot \mathbf{n}|_{\Gamma_D}]. \end{aligned} \quad (17)$$

Now the system is put into weak form considering the inner product on space $\mathcal{X} = \mathcal{L}^2(\Omega, \mathbb{R}^3) \times \mathcal{L}^2(\Omega, \mathbb{R}_{\text{sym}}^{3 \times 3})$, where \mathcal{L}^2 is the space of square integrable functions. Taking two elements $[\mathbf{a}, \mathbf{A}], [\mathbf{b}, \mathbf{B}] \in \mathcal{X}$ the inner product is computed as

$$\langle [\mathbf{a}, \mathbf{A}], [\mathbf{b}, \mathbf{B}] \rangle_{\mathcal{X}} = \int_{\Omega} \mathbf{a} \cdot \mathbf{b} \, d\Omega + \int_{\Omega} \mathbf{A} : \mathbf{B} \, d\Omega.$$

Considering a test function $\mathbf{w} = [\mathbf{w}_1, \mathbf{W}_2]$ the weak form reads

$$\langle \mathbf{w}, \mathcal{M} \partial_t \mathbf{e} \rangle_{\mathcal{X}} = \langle \mathbf{w}, \mathcal{J} \mathbf{e} \rangle_{\mathcal{X}} + \langle \mathbf{w}, \mathcal{B}_d \mathbf{u}_d \rangle_{\mathcal{X}}$$

The bilinear form $m(\mathbf{w}, \partial_t \mathbf{e}) = \langle \mathbf{w}, \mathcal{M} \partial_t \mathbf{e} \rangle_{\mathcal{X}}$ is symmetric and coercive. The bilinear form $b_d(\mathbf{w}, \mathbf{u}_d) := \langle \mathbf{w}, \mathcal{B}_d \mathbf{u}_d \rangle_{\mathcal{X}}$ takes into account distributed control.

Now an integration by parts is applied on \mathcal{J}_{Div}

$$\langle \mathbf{w}, \mathcal{J} \mathbf{e} \rangle_{\mathcal{X}} = \langle \mathbf{w}, \mathcal{J}_{\text{Grad}} \mathbf{e} \rangle_{\mathcal{X}} - \langle \mathcal{J}_{\text{Grad}} \mathbf{w}, \mathbf{e} \rangle_{\mathcal{X}} + \langle \mathbf{w}, \mathbf{u}_{\partial} \rangle_{\mathcal{L}^2(\partial\Omega)} \quad (18)$$

The expression $j_{\text{Grad}}(\mathbf{w}, \mathbf{e}) := \langle \mathbf{w}, \mathcal{J}_{\text{Grad}} \mathbf{e} \rangle_{\mathcal{X}} - \langle \mathcal{J}_{\text{Grad}} \mathbf{w}, \mathbf{e} \rangle_{\mathcal{X}}$ is a skew symmetric bilinear form as it holds $j_{\text{Grad}}(\mathbf{w}, \mathbf{e}) = -j_{\text{Grad}}(\mathbf{e}, \mathbf{w})$. The bilinear form $b_{\partial}(\mathbf{w}, \mathbf{u}_{\partial}) := \langle \mathbf{w}, \mathbf{u}_{\partial} \rangle_{\mathcal{L}^2(\partial\Omega)}$ imposes weakly the Neumann condition. System (17) is now rewritten in weak form

$$m(\mathbf{w}, \partial_t \mathbf{e}) = j_{\text{Grad}}(\mathbf{w}, \mathbf{e}) + b_d(\mathbf{w}, \mathbf{u}_d) + b_{\partial}(\mathbf{w}, \mathbf{u}_{\partial}). \quad (19)$$

In this formulation the Dirichlet boundary condition have to be imposed strongly. For this reason the test function will belong to

$$\begin{aligned} \mathbf{w}_1 &\in \mathcal{H}_{\Gamma_D}^1(\Omega, \mathbb{R}^3) := \{\mathbf{w}_1 \in \mathcal{H}^1(\Omega, \mathbb{R}^d) \mid \mathbf{w}_1|_{\Gamma_D} = 0\}, \\ \mathbf{W}_2 &\in \mathcal{L}^2(\Omega, \mathbb{R}_{\text{sym}}^{3 \times 3}), \end{aligned}$$

where \mathcal{H}^1 is the space of square integrable functions whose gradient is square integrable. The output equation is discretized considering test function w_{∂} defined over the boundary

$$\langle \mathbf{w}_{\partial}, \mathbf{y}_{\partial} \rangle_{\mathcal{X}} = \langle \mathbf{w}_{\partial}, \mathbf{e}_1 \rangle_{\mathcal{X}}. \quad (20)$$

If a Galerkin method is applied then corresponding test and trial functions are discretized using the same basis

$$\begin{aligned} \mathbf{w}_1 &= \phi_1^{\top} \mathbf{w}_1, & \mathbf{W}_2 &= \phi_2^{\top} \mathbf{w}_2, \\ \mathbf{e}_1 &= \phi_1^{\top} \mathbf{e}_1, & \mathbf{E}_2 &= \phi_2^{\top} \mathbf{e}_2, \end{aligned}$$

where, with some abuse of notation, a physical vector and the numerical vector representing its approximation are denoted in the same manner. A finite dimensional pH system is readily obtained

$$\begin{aligned} \mathbf{M} \dot{\mathbf{e}} &= \mathbf{J} \mathbf{e} + \mathbf{B}_d \mathbf{u}_d + \mathbf{B}_{\partial} \mathbf{u}_{\partial}, \\ \mathbf{y}_d &:= \mathbf{M}_d \tilde{\mathbf{y}}_d = \mathbf{B}_d^{\top} \mathbf{e}, \\ \mathbf{y}_{\partial} &:= \mathbf{M}_{\partial} \tilde{\mathbf{y}}_{\partial} = \mathbf{B}_{\partial}^{\top} \mathbf{e}. \end{aligned} \quad (21)$$

Vectors $\tilde{\mathbf{y}}_d, \tilde{\mathbf{y}}_{\partial}$ correspond to the output degrees of freedom. The outputs $\mathbf{y}_d, \mathbf{y}_{\partial}$ have been defined incorporating the mass matrix in order get the discrete power balance $\dot{H}_d = \mathbf{u}_{\partial}^{\top} \mathbf{y}_{\partial} + \mathbf{u}_d^{\top} \mathbf{y}_d$.

Remark 3 Stable mixed finite elements for the elastodynamics problem are detailed in [2]. However the formulation therein is based on a weak form obtained by integration by parts of the $\mathcal{J}_{\text{Grad}}$ operator. The mixed finite element method for such a problem are then stable in the sense of Brezzi thanks to the properties of L^2/H^{Div} finite element spaces.

4.2 Discretized rigid-flexible port-Hamiltonian dynamics

The same methodology is applied to system (14). If corresponding test functions w , state e and the effort functions z are discretized using the same bases

$$\mathbf{w} = \phi^{\top} \mathbf{w}, \quad \mathbf{e} = \phi^{\top} \mathbf{e}, \quad \mathbf{z} = \phi^{\top} \mathbf{z},$$

then a finite-dimensional pHDAE system is obtained (after integration by parts of the \mathcal{J}_{Div} operator as)

$$\begin{aligned} \mathbf{E}(\mathbf{e})\dot{\mathbf{e}} &= \mathbf{J}(\mathbf{e})\mathbf{z}(\mathbf{e}) + \mathbf{B}_d(\mathbf{e})\mathbf{u}_d + \mathbf{B}_\partial(\mathbf{e})\mathbf{u}_\partial, \\ \mathbf{y}_d &:= \mathbf{M}_d\tilde{\mathbf{y}}_d = \mathbf{B}_d^\top \mathbf{z}(\mathbf{e}), \\ \mathbf{y}_\partial &:= \mathbf{M}_\partial\tilde{\mathbf{y}}_\partial = \mathbf{B}_\partial^\top \mathbf{z}(\mathbf{e}). \end{aligned} \quad (22)$$

The computation of vector \mathbf{z} is based on the gradient of the discrete Hamiltonian:

$$\frac{\partial H_d}{\partial \mathbf{e}} = \mathbf{E}^\top \mathbf{z}, \quad H_d = H_{d,\text{kin}} + H_{d,\text{def}} + H_{d,\text{pot}},$$

For the deformation and kinetic energy it is straightforward to find the between the state and effort functions as those energy are quadratic in the state variable:

$$H_{d,\text{kin}} + H_{d,\text{def}} = \frac{1}{2} \mathbf{e}_{\text{kd}}^\top \mathbf{M}_{\text{kd}} \mathbf{e}_{\text{kd}} \longrightarrow \mathbf{z}_{\text{kd}} = \mathbf{e}_{\text{kd}}, \quad (23)$$

where $\mathbf{e}_{\text{kd}} = [\mathbf{v}_P; \boldsymbol{\omega}_P; \mathbf{v}_f; \boldsymbol{\Sigma}]$ and \mathbf{M}_{kd} is the discretization of the mass operator \mathcal{M} given in Eq (10). The only term that requires additional care is the potential energy and particularly the variational derivative of the Hamiltonian with respect to the deformation displacement $\mathbf{z}_u = \delta_{\mathbf{u}_f} H$. Consider the continuous power balance associate to

$$\dot{H} = \int_{\Omega} \frac{\partial \mathbf{u}_f}{\partial t} \cdot \mathbf{z}_u \, d\Omega = \int_{\Omega} \frac{\partial \mathbf{u}_f}{\partial t} \cdot \frac{\delta H}{\delta \mathbf{u}_f} \, d\Omega$$

The deformation velocity and its corresponding effort variable are discretized using the same basis, i.e. $\mathbf{u}_f = \boldsymbol{\phi}_u^\top \mathbf{u}_f$, $\mathbf{z}_u = \boldsymbol{\phi}_u^\top \mathbf{z}_u$. The discrete Hamiltonian rate assumes two equivalent expressions

$$\dot{H}_d(\mathbf{u}_f) = \begin{cases} \dot{\mathbf{u}}_f^\top \mathbf{M}_u \mathbf{z}_u, \\ \dot{\mathbf{u}}_f^\top \frac{\partial H_d}{\partial \mathbf{u}_f}, \end{cases}$$

where $\mathbf{M}_u = \int_{\Omega} \boldsymbol{\phi}_u \boldsymbol{\phi}_u^\top \, d\Omega$. To preserve the power balance at a discrete level it must hold $\mathbf{z}_u = \mathbf{M}_u^{-1} \frac{\partial H_d}{\partial \mathbf{u}_f}$.

Remark 4 The set Γ_D for the Dirichlet condition has to be non empty cause otherwise the deformation field is allowed for rigid movement leading to a singular mass matrix.

4.3 Application to thin planar beams

If a thin planar flexible beams is considered as mechanical model. P is placed at the origin of the local frame, while C is the ending point of the beam (see Fig. 2). The beam has length L , Young modulus E , density ρ , cross section A and second

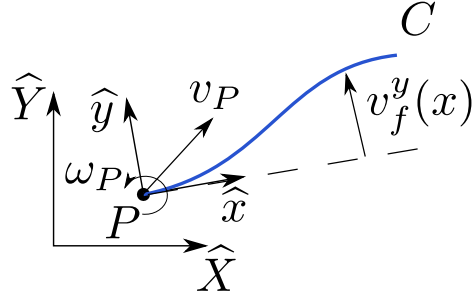


Fig. 2 Floating beam. The rigid motion is located at point P

moment of area I . The model in strong form for a flexible beam is then written compactly as

$$\begin{aligned} \begin{bmatrix} I & 0 \\ 0 & \mathcal{M} \end{bmatrix} \begin{bmatrix} \dot{\mathbf{q}} \\ \dot{\mathbf{e}} \end{bmatrix} &= \begin{bmatrix} 0 & \mathcal{J}_{qe} \\ -\mathcal{J}_{qe}^* & \mathcal{J}_e \end{bmatrix} \begin{bmatrix} \partial_{\mathbf{q}} H \\ \mathbf{e} \end{bmatrix} + \begin{bmatrix} 0 \\ \mathcal{B}_r \end{bmatrix} \mathbf{u}_{\partial}, \\ \mathbf{u}_{\partial} &= \mathcal{B}_{\partial} \mathbf{e}, \\ \mathbf{y}_{\partial} &= \mathcal{C}_{\partial} \mathbf{e}, \end{aligned} \quad (24)$$

where \mathbf{q} represents the vector of generalized coordinates $\mathbf{q} = [{}^i \mathbf{r}_P; \mathbf{R}_v; \mathbf{u}_f]$. Furthermore, the deformation field has to be constrained, to prevent rigid movement (see Rmk. 4). The appropriate selection of the boundary condition for the deformation field is an avoidable problem that depends on the particular problem under consideration. Depending on the application cantilever or simply supported boundary conditions may be considered (see Sec. §6)

$$\text{Cantilever} \begin{cases} u_f^x(x=0) &= 0, \\ u_f^y(x=0) &= 0, \\ \partial_x u_f^y(x=0) &= 0, \end{cases} \quad \text{Simply supported} \begin{cases} u_f^x(x=0) &= 0, \\ u_f^y(x=0) &= 0, \\ u_f^y(x=L) &= 0, \end{cases}$$

The state and boundary vectors are expressed as

$$\begin{aligned} \mathbf{e} &= [v_P^x, v_P^y, \omega_P^z, v_f^x, v_f^y, n_x, m_{xx}]^{\top}, \\ \mathbf{u}_{\partial} &= [F_P^x, F_P^y, T_P^z, F_C^x, F_C^y, T_C^z]^{\top}, \\ \mathbf{y}_{\partial} &= [v_P^x, v_P^y, \omega_P^z, v_C^x, v_C^y, \omega_C^z]^{\top}. \end{aligned}$$

The state contains the linear and angular velocity v_P^x, v_P^y, ω_P^z at point P , the deformation velocity v_f^x, v_f^y and the traction and bending stress n_x, m_{xx} . The boundary input contains the forces and torques acting at the extremities of the beam, while the boundary output contains the velocities at the extremities of the beam. The cross product are then adapted to the planar case. The mass operator

then reads

$$\mathcal{M} = \begin{bmatrix} \mathcal{M}_{rr} & \mathcal{M}_{rf} \\ \mathcal{M}_{fr} & \mathcal{M}_{ff} \end{bmatrix} = \begin{bmatrix} m & 0 & 0 & \mathcal{I}_\rho^L & 0 & 0 & 0 \\ 0 & m & s^x & 0 & \mathcal{I}_\rho^L & 0 & 0 \\ 0 & s^x & J^{zz} & 0 & \mathcal{I}_{\rho x}^L & 0 & 0 \\ (\bar{\mathcal{I}}_\rho^L)^* & 0 & 0 & \rho A & 0 & 0 & 0 \\ 0 & (\mathcal{I}_\rho^L)^* & (\mathcal{I}_{\rho x}^L)^* & 0 & \rho A & 0 & 0 \\ 0 & 0 & 0 & 0 & 0 & EA^{-1} & 0 \\ 0 & 0 & 0 & 0 & 0 & 0 & EI^{-1} \end{bmatrix}, \quad (25)$$

where $s^x = \int_0^L \rho A x \, dx$ is the static moment, $J^{zz} = \int_0^L \rho A x^2 \, dx$ is the moment of inertia, $\mathcal{I}_\rho^L := \int_0^L \rho A(\cdot) \, dx$, $\mathcal{I}_{\rho x}^L := \int_0^L \rho A x(\cdot) \, dx$. The interconnection operator

$$\mathcal{J}(e) = \begin{bmatrix} \mathcal{J}_{rr} & \mathcal{J}_{rf} \\ \mathcal{J}_{fr} & \mathcal{J}_{ff} \end{bmatrix} = \begin{bmatrix} 0 & 0 & +\tilde{p}_t^y & 0 & 0 & 0 & 0 \\ 0 & 0 & -\tilde{p}_t^x & 0 & 0 & 0 & 0 \\ -\tilde{p}_t^y & +\tilde{p}_t^x & 0 & -\mathcal{I}_{p_f^y}^L & +\mathcal{I}_{p_f^x}^L & 0 & 0 \\ 0 & 0 & +(\bar{\mathcal{I}}_{p_f^y}^L)^* & 0 & 0 & \partial_x & 0 \\ 0 & 0 & -(\mathcal{I}_{p_f^x}^L)^* & 0 & 0 & 0 & -\partial_{xx} \\ 0 & 0 & 0 & \partial_x & 0 & 0 & 0 \\ 0 & 0 & 0 & 0 & \partial_{xx} & 0 & 0 \end{bmatrix} \quad (26)$$

where $\tilde{p}_t^x, \tilde{p}_t^y$ are the modified canonical momenta components (see (13)), $\mathcal{I}_{p_f^x}^L := \int_0^L \{2p_f^x + \rho A v_f^x\}(\cdot) \, dx$ and $\mathcal{I}_{p_f^y}^L := \int_0^L \{2p_f^y + \rho A v_f^y\}(\cdot) \, dx$. The control operators read

$$\mathcal{B}_r = \begin{bmatrix} I_{3 \times 3} & \tau_{CP}^\top \\ 0_{4 \times 3} & 0_{4 \times 3} \end{bmatrix} \quad \text{with} \quad \tau_{CP} = \begin{bmatrix} 1 & 0 & 0 \\ 0 & 1 & L \\ 0 & 0 & 1 \end{bmatrix}, \quad (27)$$

The discretization procedure detailed in §4 is easily extended to this case considering that the differential operators here are

$$\mathcal{J}_{\text{Div}} = \begin{bmatrix} 0 & 0 & \partial_x & 0 \\ 0 & 0 & 0 & -\partial_{xx} \\ 0 & 0 & 0 & 0 \\ 0 & 0 & 0 & 0 \end{bmatrix}, \quad \mathcal{J}_{\text{Grad}} = \begin{bmatrix} 0 & 0 & 0 & 0 \\ 0 & 0 & 0 & 0 \\ \partial_x & 0 & 0 & 0 \\ 0 & \partial_{xx} & 0 & 0 \end{bmatrix}$$

The first line and second line are integrated by parts once and twice respectively, so that the boundary forces and momenta are naturally included in the discretized system as inputs. The finite-dimensional system then reads

$$\begin{bmatrix} \mathbf{I} & 0 & 0 \\ 0 & \mathbf{M}_{rr} & \mathbf{M}_{rf} \\ 0 & \mathbf{M}_{fr} & \mathbf{M}_{ff} \end{bmatrix} \begin{bmatrix} \dot{\mathbf{q}} \\ \dot{\mathbf{e}}_r \\ \dot{\mathbf{e}}_f \end{bmatrix} = \begin{bmatrix} 0 & \mathbf{J}_{qr}(\mathbf{q}) & \mathbf{J}_{qf} \\ \mathbf{J}_{rq}(\mathbf{q}) & \mathbf{J}_{rr}(\mathbf{e}) & \mathbf{J}_{rf}(\mathbf{e}) \\ \mathbf{J}_{fq} & \mathbf{J}_{fr}(\mathbf{e}) & \mathbf{J}_{ff}(\mathbf{e}) \end{bmatrix} \begin{bmatrix} \partial_{\mathbf{q}} H \\ \mathbf{e}_r \\ \mathbf{e}_f \end{bmatrix} + \begin{bmatrix} 0 \\ \mathbf{B}_{\partial,r} \\ \mathbf{B}_{\partial,f} \end{bmatrix} \mathbf{u}_\partial, \quad (28)$$

$$\mathbf{y}_\partial = \begin{bmatrix} 0 & \mathbf{B}_{\partial,r}^\top & \mathbf{B}_{\partial,f}^\top \end{bmatrix} \begin{bmatrix} \mathbf{q} \\ \mathbf{e}_r \\ \mathbf{e}_f \end{bmatrix},$$

This model describes the motion of a flexible floating beam that undergoes small deformations.

5 Multibody systems in pH form

In Sections §3, §4 the pH formulation of a single flexible floating body in infinite- and finite-dimensional form were presented. The construction of a multibody system is accomplished by exploiting the modularity of the port-Hamiltonian framework. Each element of the system is interconnected to the others by means of classical pH interconnections.

5.1 Interconnections of pHDAE systems

Consider two generic pHDAE systems of the form

$$\begin{cases} \mathbf{M}_i \dot{\mathbf{e}}_i = \mathbf{J}_i \mathbf{z}_i(\mathbf{e}_i) + \mathbf{B}_i^{\text{int}} \mathbf{u}_i^{\text{int}} + \mathbf{B}_i^{\text{ext}} \mathbf{u}_i^{\text{ext}} \\ \mathbf{y}_i = \mathbf{B}_i^T \mathbf{z}_i \end{cases} \quad \forall i = 1, 2. \quad (29)$$

where $\partial_{\mathbf{e}_i} H_i = \mathbf{M}_i^\top \mathbf{z}_i$. Systems of this kind arise from the discretization of formulation (14). The interconnection uses the internal control $\mathbf{u}_i^{\text{int}}$. An interconnection is said to be power preserving if and only if the following holds:

$$\langle \mathbf{u}_1^{\text{int}}, \mathbf{y}_1^{\text{int}} \rangle + \langle \mathbf{u}_2^{\text{int}}, \mathbf{y}_2^{\text{int}} \rangle = 0. \quad (30)$$

The power going out from one system flows in the other in a lossless manner. Two main interconnections of this kind are of interest when coupling system: the gyrator and transformer interconnection.

Gyrator interconnection The gyrator interconnection reads

$$\mathbf{u}_1^{\text{int}} = -\mathbf{C} \mathbf{y}_2^{\text{int}}, \quad \mathbf{u}_2^{\text{int}} = \mathbf{C}^\top \mathbf{y}_1^{\text{int}}.$$

This interconnection verifies (30). It is easy to verify that from this interconnection, it is obtained

$$\begin{aligned} \begin{bmatrix} \mathbf{M}_1 & 0 \\ 0 & \mathbf{M}_2 \end{bmatrix} \begin{bmatrix} \dot{\mathbf{e}}_1 \\ \dot{\mathbf{e}}_2 \end{bmatrix} &= \begin{bmatrix} \mathbf{J}_1 & -\mathbf{B}_1^{\text{int}} \mathbf{C} \mathbf{B}_2^{\text{int}\top} \\ \mathbf{B}_2^{\text{int}} \mathbf{C} \mathbf{B}_1^{\text{int}\top} & \mathbf{J}_2 \end{bmatrix} \begin{bmatrix} \mathbf{z}_1 \\ \mathbf{z}_2 \end{bmatrix} + \begin{bmatrix} \mathbf{B}_1^{\text{ext}} & 0 \\ 0 & \mathbf{B}_2^{\text{ext}} \end{bmatrix} \begin{bmatrix} \mathbf{u}_1^{\text{ext}} \\ \mathbf{u}_2^{\text{ext}} \end{bmatrix} \\ \begin{bmatrix} \mathbf{y}_1^{\text{ext}} \\ \mathbf{y}_2^{\text{ext}} \end{bmatrix} &= \begin{bmatrix} \mathbf{B}_1^{\text{ext}\top} & 0 \\ 0 & \mathbf{B}_2^{\text{ext}\top} \end{bmatrix} \begin{bmatrix} \mathbf{z}_1 \\ \mathbf{z}_2 \end{bmatrix}, \end{aligned}$$

with $H(\mathbf{e}_1, \mathbf{e}_2) = H_1(\mathbf{e}_1) + H_2(\mathbf{e}_2)$.

Transformer interconnection The transformer interconnection reads

$$\mathbf{u}_1^{\text{int}} = -\mathbf{C} \mathbf{u}_2^{\text{int}}, \quad \mathbf{y}_2^{\text{int}} = \mathbf{C}^\top \mathbf{y}_1^{\text{int}}.$$

Again, this interconnection verifies (30). After the interconnection the final system is differential algebraic:

$$\begin{aligned} \begin{bmatrix} \mathbf{M}_1 & 0 & 0 \\ 0 & \mathbf{M}_2 & 0 \\ 0 & 0 & 0 \end{bmatrix} \begin{bmatrix} \dot{\mathbf{e}}_1 \\ \dot{\mathbf{e}}_2 \\ \dot{\boldsymbol{\lambda}} \end{bmatrix} &= \begin{bmatrix} \mathbf{J}_1 & 0 & -\mathbf{B}_1^{\text{int}} \mathbf{C} \\ 0 & \mathbf{J}_2 & \mathbf{B}_2^{\text{int}} \\ \mathbf{C}^\top \mathbf{B}_1^{\text{int}\top} & -\mathbf{B}_2^{\text{int}\top} & 0 \end{bmatrix} \begin{bmatrix} \mathbf{z}_1 \\ \mathbf{z}_2 \\ \boldsymbol{\lambda} \end{bmatrix} + \begin{bmatrix} \mathbf{B}_1^{\text{ext}} & 0 \\ 0 & \mathbf{B}_2^{\text{ext}} \\ 0 & 0 \end{bmatrix} \begin{bmatrix} \mathbf{u}_1^{\text{ext}} \\ \mathbf{u}_2^{\text{ext}} \end{bmatrix} \\ \begin{bmatrix} \mathbf{y}_1^{\text{ext}} \\ \mathbf{y}_2^{\text{ext}} \end{bmatrix} &= \begin{bmatrix} \mathbf{B}_1^{\text{ext}\top} & 0 & 0 \\ 0 & \mathbf{B}_2^{\text{ext}\top} & 0 \end{bmatrix} \begin{bmatrix} \mathbf{z}_1 \\ \mathbf{z}_2 \\ \boldsymbol{\lambda} \end{bmatrix}. \end{aligned}$$

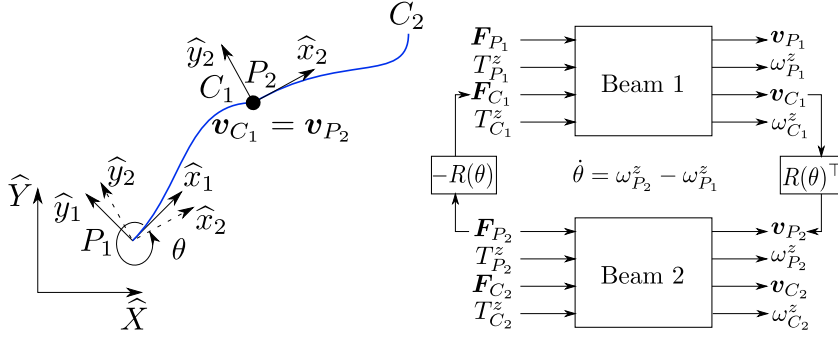


Fig. 3 Two beams interconnected by an hinge

5.2 Application to multibody systems of beams

Once a discretized system is obtained by application of a transformer interconnection lossless joints can be introduced. A common example is an hinged link between two beams. In this case the internal variables are

$$\begin{aligned} \mathbf{u}_1^{\text{int}} &= [F_{C_1}^x, F_{C_1}^y]^\top := \mathbf{F}_{C_1}, & \mathbf{y}_1^{\text{int}} &= [v_{C_1}^x, v_{C_1}^y]^\top := \mathbf{v}_{C_1}, \\ \mathbf{u}_2^{\text{int}} &= [F_{P_2}^x, F_{P_2}^y]^\top := \mathbf{F}_{P_2}, & \mathbf{y}_2^{\text{int}} &= [v_{P_2}^x, v_{P_2}^y]^\top := \mathbf{v}_{P_2}. \end{aligned}$$

The interconnection matrix is the relative rotation matrix between the two local frames

$$\mathbf{R}(\theta) = \begin{bmatrix} \cos(\theta) & -\sin(\theta) \\ \sin(\theta) & \cos(\theta) \end{bmatrix}, \quad \theta(t) = \theta(0) + \int_0^t (\omega_{P_2}^z - \omega_{P_1}^z) \, d\tau. \quad (31)$$

The transformer interconnection

$$\mathbf{F}_{C_1} = -\mathbf{R}(\theta)\mathbf{F}_{P_2}, \quad \mathbf{v}_{P_2} = \mathbf{R}(\theta)^\top \mathbf{v}_{C_1}. \quad (32)$$

imposes the constraints on a velocity level and gives rise to a quasi-linear index 2 pHDAE:

$$\begin{aligned} \begin{bmatrix} \mathbf{M}_1 & 0 & 0 \\ 0 & \mathbf{M}_2 & 0 \\ 0 & 0 & 0 \end{bmatrix} \begin{bmatrix} \dot{\mathbf{e}}_1 \\ \dot{\mathbf{e}}_2 \\ \dot{\boldsymbol{\lambda}} \end{bmatrix} &= \begin{bmatrix} \mathbf{J}_1(\mathbf{e}_1) & 0 & -\mathbf{B}_1^{\text{int}} \mathbf{R} \\ 0 & \mathbf{J}_2(\mathbf{e}_2) & \mathbf{B}_2^{\text{int}} \\ \mathbf{R}^\top \mathbf{B}_1^{\text{int}\top} & -\mathbf{B}_2^{\text{int}\top} & 0 \end{bmatrix} \begin{bmatrix} \mathbf{z}_1 \\ \mathbf{z}_2 \\ \boldsymbol{\lambda} \end{bmatrix} + \begin{bmatrix} \mathbf{B}_{\partial 1}^{\text{ext}} & 0 \\ 0 & \mathbf{B}_{\partial 2}^{\text{ext}} \\ 0 & 0 \end{bmatrix} \begin{bmatrix} \mathbf{u}_1^{\text{ext}} \\ \mathbf{u}_2^{\text{ext}} \end{bmatrix} \\ \begin{bmatrix} \mathbf{y}_1^{\text{ext}} \\ \mathbf{y}_2^{\text{ext}} \end{bmatrix} &= \begin{bmatrix} \mathbf{B}_{\partial 1}^{\text{ext}\top} & 0 & 0 \\ 0 & \mathbf{B}_{\partial 2}^{\text{ext}\top} & 0 \end{bmatrix} \begin{bmatrix} \mathbf{z}_1 \\ \mathbf{z}_2 \\ \boldsymbol{\lambda} \end{bmatrix}. \end{aligned} \quad (33)$$

A transformer interconnection is indeed equivalent to a gyrator interconnection of pHDAE systems. It is sufficient to interchange the role of output and input of the second system $\mathbf{u}_2^{\text{int}} \leftrightarrow \mathbf{y}_2^{\text{int}}$. The output then plays the role of a Lagrange multiplier. Thus one may use SIMULINK[®] to interconnect pHDAE using an equivalent gyrator interconnection.

This approach allow to modularly construct multibody systems of arbitrary complexity. Other kind of lossless joints (prismatic, spherical) can be modeled by appropriate interconnections. The system can then be simulated by using specific DAE solvers [4] or appropriately reduced to get an ordinary differential equation. The port-Hamiltonian structure is preserved if a null space matrix is employed to eliminate the Lagrange multiplier. Consider a generic pHDAE where the differential and algebraic part are explicitly separated

$$\begin{aligned} M\dot{e} &= J(e)z(e) + G^\top(e)\lambda + Bu, \\ 0 &= G(e)z(e), \end{aligned} \quad (34)$$

and matrix $P(e)$ that satisfies

$$\text{range}\{P(e)\} = \text{null}\{G(e)\},$$

then the admissible variable belongs to the range of P , considering the transformations $\hat{z} = Pz$, $\hat{e} = Pe$ and pre-multiplying the system by P^\top an equivalent ODE is obtained

$$\widehat{M}(\hat{e})\dot{\hat{e}} = \widehat{J}(\hat{e})\hat{z}(\hat{e}) + \widehat{B}(\hat{e})u,$$

with $\widehat{M} = P^\top MP$, $\widehat{J} = P^\top JP$, $\widehat{B} = P^\top B$. The actual computation of P can be obtained by QR decomposition of matrix G [20]. Once an equivalent ODE formulation is obtained the concepts and ideas presented in [10] can be used to reduce the flexible dynamics.

5.3 The linear case: sub-structuring and model reduction

If the angular velocities and the relative orientations are small then the system may be linearized about a particular geometrical configuration. Omitting the partition related to the generalized coordinates and dividing the system into rigid and flexible dynamics, the resulting equations are then expressed as

$$\begin{bmatrix} M_{rr} & M_{rf} & 0 \\ M_{fr} & M_{ff} & 0 \\ 0 & 0 & 0 \end{bmatrix} \begin{bmatrix} \dot{e}_r \\ \dot{e}_f \\ \lambda \end{bmatrix} = \begin{bmatrix} 0 & 0 & G_r^\top \\ 0 & J_{ff} & G_f^\top \\ -G_r & -G_f & 0 \end{bmatrix} \begin{bmatrix} e_r \\ e_f \\ \lambda \end{bmatrix} + \begin{bmatrix} B_r \\ B_f \\ 0 \end{bmatrix} u, \quad (35)$$

The Hamiltonian is now a quadratic function of the state variables $H = \frac{1}{2}e^\top Me$ [3]. The modular construction of complex multi-body systems than is analogous to a sub-structuring technique [19] where the velocities and forces are linked at the interconnection points. Such system can be reduced using Krilov subspace method directly on the DAE formulation [13]. The basic idea relies on the construction of a subspace V_f^{red} for the vector e_f such that $e_f \approx V_f^{\text{red}} e_f^{\text{red}}$. The reduced system then reads

$$\begin{bmatrix} M_{rr} & M_{rf}^{\text{red}} & 0 \\ M_{fr}^{\text{red}} & M_{ff}^{\text{red}} & 0 \\ 0 & 0 & 0 \end{bmatrix} \begin{bmatrix} \dot{e}_r \\ \dot{e}_f^{\text{red}} \\ \lambda \end{bmatrix} = \begin{bmatrix} 0 & 0 & G_r^\top \\ 0 & J_{ff}^{\text{red}} & G_f^{\text{red}\top} \\ -G_r & -G_f^{\text{red}} & 0 \end{bmatrix} \begin{bmatrix} e_r \\ e_f^{\text{red}} \\ \lambda \end{bmatrix} + \begin{bmatrix} B_r \\ B_f^{\text{red}} \\ 0 \end{bmatrix} u, \quad (36)$$

where the second equation has been pre-multiplied by $V_f^{\text{red}\top}$.

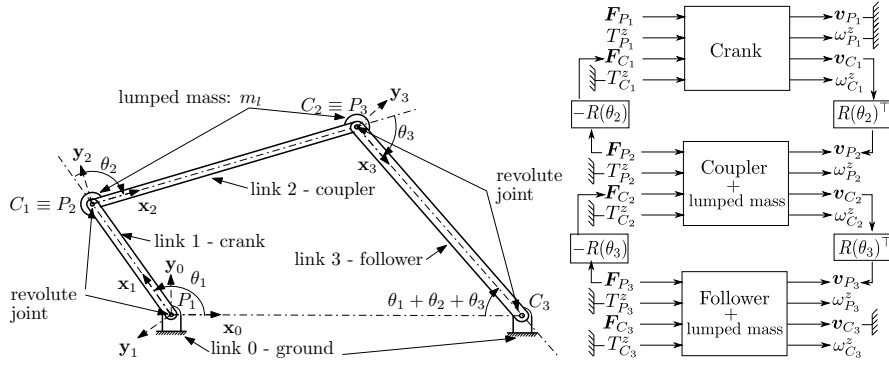


Fig. 4 Four bar mechanism illustration (left, taken from [11]) and block diagram used for the eigenvalues analysis (right)

Table 1 Four-bar mechanism links properties: each link is a uniform beam with mass density $\rho = 2714 \text{ kg/m}^3$ and Young modulus $E = 7.1 \cdot 10^{10} \text{ N/m}^2$. The lumped masses $m_l = 0.042 \text{ kg}$ are taken into account considering an additional mass at P for link 2 and 3.

i	0	1	2	3
Name	ground	crank	coupler	follower
Length L_i (m)	0.254	0.108	0.2794	0.2705
Cross section A_i (m^2)	—	$1.0774 \cdot 10^{-4}$	$4.0645 \cdot 10^{-5}$	$4.0645 \cdot 10^{-5}$
Flexural rigidity $(EI)_i$ (Nm^2)	—	11.472	0.616	0.616

6 Validation

In this section numerical simulations are performed to assess the correctness of the proposed formulation. A first example concerns the computation of eigenvalues of a four bar mechanism for different geometrical configurations. The second example is a rotating crank-slider. In this case the non-linearities cannot be neglected. The third example is a beam hinged and undergoing external excitations so that the out of plane motion becomes important. The following examples make use of Euler Bernoulli beam model (28). To discretize the system Lagrange polynomials of order one are used for v_f^x and n_x , while Hermite polynomials are used for v_f^y and m_{xx} . This choice ensures the conformity with respect to the differential operator. The Firedrake python library [27] is employed to construct the finite dimensional discretization.

6.1 Linear analysis of a four-bar mechanism

The four-bar mechanism has one degree of freedom and represents a closed chain of rigid bodies. The data taken from [18, 11] are recalled in Table 1. In Fig. 4 the mechanism and the corresponding block diagram used for constructing the final PH system are presented. The lumped masses are directly included in the coupler and follower model considering a simple modification to the rigid mass matrix

$$\mathbf{M}_{rr}^{i+m_l}[1:2, 1:2] = \mathbf{M}_{rr}^i[1:2, 1:2] + \mathbf{I}_{2 \times 2} m_l, \quad (37)$$

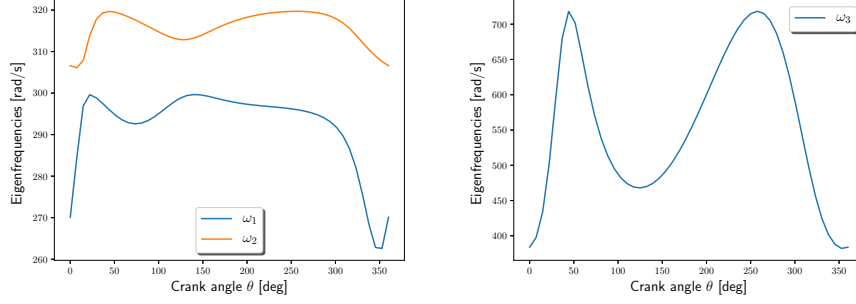


Fig. 5 Eigenvalues ω_i , $i = 1, 2, 3$ for the four bar mechanism for varying crank angle.

where $i = 2, 3$ denotes the coupler or follower model. Given a certain crank angle θ_1 the relative angles between the different links are found by solving the two kinematic constraint

$$\begin{aligned} L_1 \cos(\theta_1) + L_2 \cos(\theta_1 + \theta_2) + L_3 \cos(\theta_1 + \theta_2 + \theta_3) &= L_0, \\ L_1 \sin(\theta_1) + L_2 \sin(\theta_1 + \theta_2) + L_3 \sin(\theta_1 + \theta_2 + \theta_3) &= 0. \end{aligned}$$

Once the geometrical configuration the transformer interconnection (32) is applied to insert a revolute joint between adjacent links. For the deformation field a cantilever condition is imposed for each beam. The resulting system is the constrained to ground by imposing to following equalities

$$\mathbf{v}_{P_1} = 0, \quad \omega_{P_1}^z = 0, \quad \mathbf{v}_{C_3} = 0.$$

The resulting system is expressed in pH form as $\mathbf{E}\dot{\mathbf{e}} = \mathbf{J}\mathbf{e}$. The eigenfrequencies are then found by solving the generalized eigenvalue problem $\mathbf{E}\Phi = \mathbf{J}\Phi\Lambda$. Since \mathbf{J} is skew-symmetric the eigenvalues will be imaginary $\lambda = j\Omega$. The first three pulsations are reported in 5 for different values of the crank angle θ_1 . The results match perfectly [18,11], assessing the validity of the linear model.

6.2 Rotating crank-slider

To verify the non-linear planar model a crank-slider rotating at high speed is considered. The example is retrieved from [14]. The crank is considered as rigid, with length $L_{cr} = 0.15$ m and rotates at a constant angular rate $\omega_{cr} = 150$ rad/s. The flexible coupler has length $L_{cl} = 0.3$ [m] and a circular cross section whose diameter is $d_{cl} = 6$ mm. Its Young modulus and density are given by $E_{cl} = 0.2 \cdot 10^{12}$ Pa, $\rho_{cl} = 7870$ kg/m³. The slider has a total mass equal to half the mass of the coupler $m_{sl} = 0.033$ kg. A simply supported condition is supposed for the coupler deformation field. This choice is motivated by the fact that the slider has a large inertia and does not allow elastic displacement at the tip.

An illustration of the system and the block diagram used to construct the model are provided in Fig. 6. To construct the crank slider a transformer interconnection is first used to connect the slider to the flexible coupler. The motion of the slider is then computed in the coupler reference frame. Then the sliding constraint, that

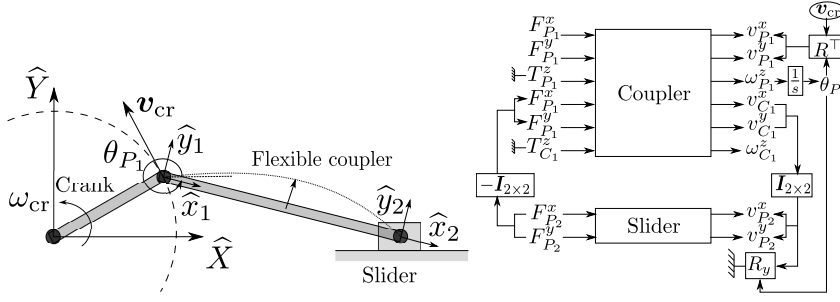


Fig. 6 Crank slider illustration (left) and block diagram (right)

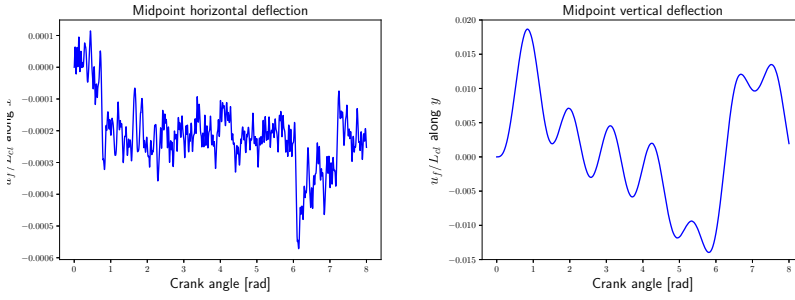


Fig. 7 Coupler midpoint horizontal (left) and vertical (right) displacement

requires the vertical velocity of the slider to be null in the inertial frame, is imposed as follows

$$0 = \sin(\theta_{P_1})v_{P_2}^x + \cos(\theta_{P_1})v_{P_2}^y = \mathbf{R}_y(\theta_{P_1})\mathbf{v}_{P_2},$$

where \mathbf{R}_y is the second line of the rotation matrix and $\dot{\theta}_{P_1} = \omega_{P_1}^z$ is the angle defining the orientation of the coupler. The rigid crank velocity at the endpoint

$$\mathbf{v}_{cr}(t) = -\omega_{cr}L_{cr}\sin(\omega_{cr}t)\hat{\mathbf{X}} + \omega_{cr}L_{cr}\cos(\omega_{cr}t)\hat{\mathbf{Y}}$$

has to be written in the coupler reference frame to get the input

$$\mathbf{u}_{cl} = \mathbf{R}(\theta_{P_1})^\top \mathbf{v}_{cr}. \quad (38)$$

The resulting system is a quasi linear index-2 DAE of the form

$$\begin{bmatrix} \mathbf{M} & \mathbf{0} & \mathbf{0} \\ \mathbf{0} & \mathbf{0} & \mathbf{0} \\ \mathbf{0} & \mathbf{0} & \mathbf{0} \end{bmatrix} \begin{bmatrix} \dot{\mathbf{e}} \\ \dot{\boldsymbol{\lambda}}_0 \\ \dot{\boldsymbol{\lambda}}_u \end{bmatrix} + \begin{bmatrix} \mathbf{J}(\mathbf{e}) & \mathbf{G}_0^\top(\theta_{P_1}) & \mathbf{G}_u^\top \\ -\mathbf{G}_0(\theta_{P_1}) & \mathbf{0} & \mathbf{0} \\ -\mathbf{G}_u & \mathbf{0} & \mathbf{0} \end{bmatrix} \begin{bmatrix} \mathbf{e} \\ \boldsymbol{\lambda}_0 \\ \boldsymbol{\lambda}_u \end{bmatrix} + \begin{bmatrix} \mathbf{0} \\ \mathbf{0} \\ \mathbf{R}(\theta_{P_1})^\top \end{bmatrix} \mathbf{v}_{cr}$$

Setting properly initial condition is of crucial importance for a DAE solver. For this problem the beam is supposed undeformed at the initial time. The initial conditions for the rigid movement are then found using basic kinematics considerations. The system is then solved using the IDA algorithm available in the Assimulo library [1]. In Fig. 7 the midpoint deformation displacement $u_f^x(L_{cl}/2)$, $u_f^y(L_{cl}/2)$, normalized with respect to the coupler length, is reported. The resulting vertical displacement is in accordance with the results presented in [14]. The horizontal

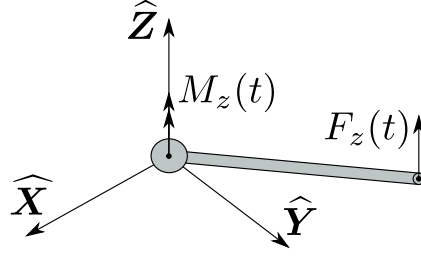


Fig. 8 Spatial beam on a spherical joint.

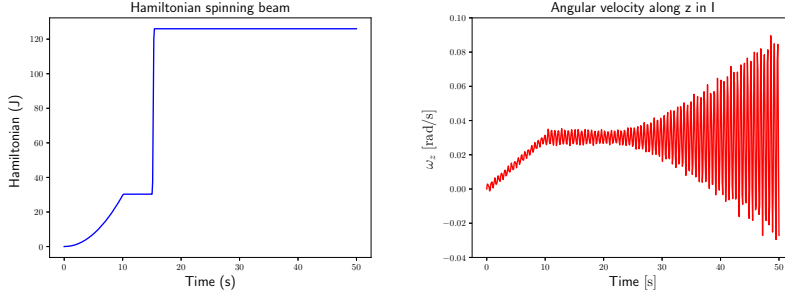


Fig. 9 Simulation results: kinetic energy (left) and angular velocity about the vertical inertial direction (right).

displacement exhibits high oscillations because of the higher eigenfrequencies of the longitudinal movement. This is due to the fact that the initial condition is not the one required by a smoother solution [29]. The initial deformation has to be computed from the rigid initial condition.

6.3 Hinged spatial beam

A spatial beam rotating about a spherical joint is considered. This example was considered in [7, 14]. The physical parameters are briefly recalled in Table 2. The spherical joint constraint is imposed by setting to zero the linear velocity, while a cantilever is imposed for the deformation field as the tip is free. For the first 10.2[s] a torque of 200 [N/mm] is applied about the vertical axis. Then an impulsive force of [N] is applied at the tip of the beam, to excite the out-of-plane movement. In Fig. 8 an illustration of the mechanical model is shown. The system is solved using an implicit Runge-Kutta method of the Radau IIA family. The simulation results, provided in Fig. 9, corresponds to the Kinetic energy and the angular velocity measured in the inertial vertical direction. The result matches with the provided references and the energy. Indeed the non linearities associated to the gyroscopic terms are small as the maximum angular velocity is equal to 0.1 rad/s \approx 5 deg/s.

Table 2 Physical parameters for the hinged spatial beam.

Length	Cross section	Inertia moment	Density	Young modulus
141.45 [mm]	9.0 [mm ²]	6.75 [mm ⁴]	7800 [kg/mm ³]	2.1 10 ⁶ [N/m ²]

7 Conclusion

A port-Hamiltonian formulation for the flexible multibody dynamics has been discussed. The proposed methodology, being based on a floating frame formulation, relies on the hypothesis of small deformations. The inclusion of the geometric stiffening is possible and will be investigated. The discretization procedure uses a mixed finite element method, hence, the stress distribution is available without any post-processing. This is a valuable characteristic of this framework as the stress distribution is the most important variable for preliminary analysis of mechanical components. Moreover, this approach allows to include higher dimensional problem easily (e.g. plates, shells). However, the stability and numerical convergence of the associated finite element has to be proved. Another interesting topic is the application of model reduction techniques. While for linear pHDAE systems consolidated methodologies exist, for the general non linear differential-algebraic case, generic solutions are not yet available. The index reduction strategies for differential algebraic system can make the problem purely differential, eliminating the issues due to the algebraic part. The pH framework is well suited for control applications and the incorporation of control strategies is an important topic to be explored in the future.

Appendix 1: Detailed derivation of the equation of motions

The detailed derivation of the pH system (12) is here presented. First, let us recall the equations for a floating flexible body reported in [29, 30].

Linear momentum balance:

$$m^i \ddot{\mathbf{r}}_P + \mathbf{R}[\mathbf{s}_u]^\top \dot{\boldsymbol{\omega}}_P + \mathbf{R} \int_{\Omega} \rho \ddot{\mathbf{u}}_f \, d\Omega = \\ + \mathbf{R} \left\{ -[\boldsymbol{\omega}_P] \times [\boldsymbol{\omega}_P] \times \mathbf{s}_u - \int_{\Omega} 2\rho [\boldsymbol{\omega}_P] \times \dot{\mathbf{u}}_f \, d\Omega + \int_{\Omega} \boldsymbol{\beta} \, d\Omega + \int_{\partial\Omega} \boldsymbol{\tau} \, d\Gamma \right\} \quad (39)$$

Angular momentum balance:

$$[\mathbf{s}_u] \times \mathbf{R}^\top {}^i \ddot{\mathbf{r}}_P + \mathbf{J}_u \dot{\boldsymbol{\omega}}_P + \int_{\Omega} \rho [\mathbf{x} + \mathbf{u}_f] \times \ddot{\mathbf{u}}_f \, d\Omega - [\boldsymbol{\omega}_P] \times \mathbf{J}_u \boldsymbol{\omega}_P = \\ - \int_{\Omega} 2\rho [\mathbf{x} + \mathbf{u}_f] \times [\boldsymbol{\omega}_P] \times \dot{\mathbf{u}}_f \, d\Omega + \int_{\Omega} [\mathbf{x} + \mathbf{u}_f] \times \boldsymbol{\beta} \, d\Omega + \int_{\partial\Omega} [\mathbf{x} + \mathbf{u}_f] \times \boldsymbol{\tau} \, d\Gamma \quad (40)$$

Flexibility PDE:

$$\rho \mathbf{R}^\top {}^i \ddot{\mathbf{r}}_P + \rho([\dot{\boldsymbol{\omega}}_P] \times + [\boldsymbol{\omega}_P] \times [\boldsymbol{\omega}_P] \times)(\mathbf{x} + \mathbf{u}_f) + \rho(2[\boldsymbol{\omega}_P] \times \dot{\mathbf{u}}_f + \ddot{\mathbf{u}}_f) = \text{Div } \boldsymbol{\Sigma} + \boldsymbol{\beta}, \quad (41)$$

References

1. Andersson, C., Führer, C., Åkesson, J.: Assimulo: A unified framework for {ODE} solvers. *Mathematics and Computers in Simulation* **116**(0), 26 – 43 (2015). DOI <http://dx.doi.org/10.1016/j.matcom.2015.04.007>
2. Arnold, D., Lee, J.: Mixed methods for elastodynamics with weak symmetry. *SIAM Journal on Numerical Analysis* **52**(6), 2743–2769 (2014). DOI [10.1137/13095032X](https://doi.org/10.1137/13095032X)
3. Beattie, C., Mehrmann, V., Xu, H., Zwart, H.: Linear port-Hamiltonian descriptor systems. *Mathematics of Control, Signals, and Systems* **30**(4), 17 (2018)
4. Brenan, K.E., Campbell, S.L., Petzold, L.R.: *Numerical Solution of Initial-Value Problems in Differential-Algebraic Equations*. Society for Industrial and Applied Mathematics (1995). DOI [10.1137/1.9781611971224](https://doi.org/10.1137/1.9781611971224). URL <https://epubs.siam.org/doi/pdf/10.1137/1.9781611971224>
5. Brugnoli, A., Alazard, D., Pommier-Budinger, V., Matignon, D.: Port-Hamiltonian formulation and symplectic discretization of plate models part I: Mindlin model for thick plates. *Applied Mathematical Modelling* **75**, 940 – 960 (2019). DOI [10.1016/j.apm.2019.04.035](https://doi.org/10.1016/j.apm.2019.04.035). URL <https://doi.org/10.1016/j.apm.2019.04.035>
6. Brugnoli, A., Alazard, D., Pommier-Budinger, V., Matignon, D.: Port-Hamiltonian formulation and symplectic discretization of plate models part II: Kirchhoff model for thin plates. *Applied Mathematical Modelling* **75**, 961 – 981 (2019). DOI [10.1016/j.apm.2019.04.036](https://doi.org/10.1016/j.apm.2019.04.036). URL <https://doi.org/10.1016/j.apm.2019.04.036>
7. Cardona, A.: Superelements modelling in flexible multibody dynamics. *Multibody System Dynamics* **4**(2), 245–266 (2000). DOI [10.1023/A:1009875930232](https://doi.org/10.1023/A:1009875930232). URL <https://doi.org/10.1023/A:1009875930232>
8. Cardoso-Ribeiro, F.L., Matignon, D., Lefèvre, L.: A partitioned finite element method for power-preserving discretization of open systems of conservation laws. *arXiv preprint arXiv:1906.05965* (2019). Under review
9. Cervera, J., van der Schaft, A.J., Baños, A.: Interconnection of port-Hamiltonian systems and composition of dirac structures. *Automatica* **43**(2), 212–225 (2007). DOI [10.1016/j.automatica.2006.08.014](https://doi.org/10.1016/j.automatica.2006.08.014)
10. Chaturantabut, S., Beattie, C., Gugercin, S.: Structure-preserving model reduction for nonlinear port-Hamiltonian systems. *SIAM Journal on Scientific Computing* **38**(5), B837–B865 (2016). DOI [10.1137/15M1055085](https://doi.org/10.1137/15M1055085)
11. Chebbi, J., Dubanchet, V., Perez Gonzalez, J.A., Alazard, D.: Linear dynamics of flexible multibody systems. *Multibody System Dynamics* **41**(1), 75–100 (2017). DOI [10.1007/s11044-016-9559-y](https://doi.org/10.1007/s11044-016-9559-y). URL <https://doi.org/10.1007/s11044-016-9559-y>
12. Duindam, V., Macchelli, A., Stramigioli, S., Bruyninckx, H.: *Modeling and Control of Complex Physical Systems*. Springer Verlag (2009). URL <https://www.springer.com/us/book/9783642031953>
13. Egger, H., Kugler, T., Liljegren-Sailer, B., Marheineke, N., Mehrmann, V.: On structure-preserving model reduction for damped wave propagation in transport networks. *SIAM Journal on Scientific Computing* **40**(1), A331–A365 (2018). DOI [10.1137/17M1125303](https://doi.org/10.1137/17M1125303)
14. Ellenbroek, M., Schilder, J.: On the use of absolute interface coordinates in the floating frame of reference formulation for flexible multibody dynamics. *Multibody System Dynamics* **43**(3), 193–208 (2018). DOI [10.1007/s11044-017-9606-3](https://doi.org/10.1007/s11044-017-9606-3). URL <https://doi.org/10.1007/s11044-017-9606-3>
15. Forni, P., Jeltsema, D., Lopes, G.A.: Port-Hamiltonian formulation of rigid-body attitude control. *IFAC-PapersOnLine* **48**(13), 164 – 169 (2015). DOI <https://doi.org/10.1016/j.ifacol.2015.10.233>. URL <http://www.sciencedirect.com/science/article/pii/S2405896315021242>. 5th IFAC Workshop on Lagrangian and Hamiltonian Methods for Nonlinear Control LHMNC 2015
16. Golo, G., Talasila, V., van der Schaft, A.J., Maschke, B.: Hamiltonian discretization of boundary control systems. *Automatica* **40**(5), 757–771 (2004). DOI [10.1016/j.automatica.2003.12.017](https://doi.org/10.1016/j.automatica.2003.12.017). URL <http://dx.doi.org/10.1016/j.automatica.2003.12.017>
17. Hurty, W.C.: Dynamic analysis of structural systems using component modes. *AIAA Journal* **3**(4), 678–685 (1965). DOI [10.2514/3.2947](https://doi.org/10.2514/3.2947). URL <https://doi.org/10.2514/3.2947>
18. Kitis, L., Lindenberg, R.: Natural frequencies and mode shapes of flexible mechanisms by a transfer matrix method. *Finite Elements in Analysis and Design* **6**(4), 267 – 285 (1990). DOI [10.1016/0168-874X\(90\)90020-F](https://doi.org/10.1016/0168-874X(90)90020-F). URL [https://doi.org/10.1016/0168-874X\(90\)90020-F](https://doi.org/10.1016/0168-874X(90)90020-F)

19. Klerk, D.D., Rixen, D.J., Voormeeren, S.N.: General framework for dynamic substructuring: History, review and classification of techniques. *AIAA Journal* **46**(5), 1169–1181 (2008). DOI 10.2514/1.33274. URL <https://doi.org/10.2514/1.33274>
20. Leyendecker, S., Betsch, P., Steinmann, P.: The discrete null space method for the energy-consistent integration of constrained mechanical systems. part III: Flexible multibody dynamics. *Multibody System Dynamics* **19**(1), 45–72 (2008). DOI 10.1007/s11044-007-9056-4. URL <https://doi.org/10.1007/s11044-007-9056-4>
21. Macchelli, A., Melchiorri, C., Stramigioli, S.: Port-based modeling of a flexible link. *IEEE Transactions on Robotics* **23**, 650 – 660 (2007). DOI 10.1109/TRO.2007.898990
22. Macchelli, A., Melchiorri, C., Stramigioli, S.: Port-based modeling and simulation of mechanical systems with rigid and flexible links. *IEEE Transactions on Robotics* **25**(5), 1016–1029 (2009). DOI 10.1109/TRO.2009.2026504
23. Mehrmann, V., Morandin, R.: Structure-preserving discretization for port-Hamiltonian descriptor systems. arXiv preprint arXiv:1903.10451 (2019). To be presented at the 2019 IEEE Conference on Decision and Control
24. Nagesh Rao, S.P., Lopes, G.A.D., Jeltsema, D., Babuška, R.: Port-hamiltonian systems in adaptive and learning control: A survey. *IEEE Transactions on Automatic Control* **61**(5), 1223–1238 (2016). DOI 10.1109/TAC.2015.2458491
25. Nowakowski, C., Fehr, J., Fischer, M., Eberhard, P.: Model order reduction in elastic multibody systems using the floating frame of reference formulation. *IFAC Proceedings Volumes* **45**(2), 40 – 48 (2012). DOI <https://doi.org/10.3182/20120215-3-AT-3016.00007>. URL <http://www.sciencedirect.com/science/article/pii/S1474667016306401>. 7th Vienna International Conference on Mathematical Modelling
26. Ortega, R., García-Canseco, E.: Interconnection and damping assignment passivity-based control: A survey. *European Journal of Control* **10**(5), 432 – 450 (2004)
27. Rathgeber, F., Ham, D., Mitchell, L., Lange, M., Luporini, F., McRae, A.T., Bercea, G., Markall, G.R., Kelly, P.: Firedrake: automating the finite element method by composing abstractions. *ACM Transactions on Mathematical Software (TOMS)* **43**(3), 24 (2017)
28. Rui, X., He, B., Lu, Y., Lu, W., Wang, G.: Discrete time transfer matrix method for multibody system dynamics. *Multibody System Dynamics* **14**(3), 317–344 (2005). DOI 10.1007/s11044-005-5006-1. URL <https://doi.org/10.1007/s11044-005-5006-1>
29. Simeon, B.: DAEs and PDEs in elastic multibody systems. *Numerical Algorithms* **19**(1), 235–246 (1998). DOI 10.1023/A:1019118809892. URL <https://doi.org/10.1023/A:1019118809892>
30. Simeon, B.: Computational flexible multibody dynamics. Springer (2013)
31. Steinbrecher, A.: Numerical solution of quasi-linear differential-algebraic equations and industrial simulation of multibody systems. Ph.D. thesis, TU Berlin (2006). DOI 10.14279/depositonce-1360
32. Tan, T., Yousuff, A., Bahar, L., Konstantinidis, M.: A modified finite element-transfer matrix for control design of space structures. *Computers & Structures* **36**(1), 47 – 55 (1990). DOI [https://doi.org/10.1016/0045-7949\(90\)90173-Y](https://doi.org/10.1016/0045-7949(90)90173-Y). URL <http://www.sciencedirect.com/science/article/pii/004579499090173Y>
33. Wasfy, T.M., Noor, A.K.: Computational strategies for flexible multibody systems. *Applied Mechanics Reviews* **56**(6), 553–613 (2003). DOI 10.1115/1.1590354. URL https://asmedigitalcollection.asme.org/appliedmechanicsreviews/article-pdf/56/6/553/5440485/553_1.pdf
34. Yigit, A., Scott, R., Ulsoy, A.G.: Flexural motion of a radially rotating beam attached to a rigid body. *Journal of Sound and Vibration* **121**(2), 201 – 210 (1988). DOI 10.1016/S0022-460X(88)80024-5
35. Young, K.D.: Distributed finite-element modeling and control approach for large flexible structures. *Journal of Guidance, Control, and Dynamics* **13**(4), 703–713 (1990). DOI 10.2514/3.25389. URL <https://doi.org/10.2514/3.25389>